A Comparative Study between Rectangular, Circular and Annular Ring Shaped Microstrip Antennas

Jayanta Bhattacharya
Dept. of Electronics and Communication Engg
National Institute of Technology, Rourkela, Odisha – 769 008, India
jayantabhattacharya86@gmail.com

Sudipta Maity
Dept. of Electronics and Communication Engg
National Institute of Technology, Rourkela, Odisha – 769 008, India
sdpt123maity@gmail.com

Abstract—**In this paper, a comparative study between three different shaped Microstrip Antennas (MAs) which include rectangular, circular and annular ring-shaped geometries is presented. Cavity model technique is used for theoretical investigations. For comparison purpose, the areas of those three MAs are kept fixed. Eigenfunction, eigenvalue, resonant frequency and far-field radiation pattern are investigated and compared for all three antennas. The comparative study is presented for the first three modes for the first time, hitherto unreported.**

Keywords—Microstrip antenna, resonant frequency, radiation pattern, cavity model.

I. Introduction

Microstrip Antennas (MAs) become very popular for various applications due to its low profile, light weight, conformability and low cost. Numerous analytical and numerical techniques have been used over last 50 years to deduce resonant frequency, radiation characteristics etc. of various shapes of Microstrip antennas [1].

The first practical microstrip antenna patented by R. E Munson where rectangular and square microstrip antennas have been investigated using transmission line model in 1974 [2]. A. G. Denryd et al. have introduced cavity model technique and have used it to calculate the input conductance, resonant frequency, quality factor, bandwidth, far-field patterns, etc. for Rectangular Microstrip Antenna (RMA) [3, 4]. In 1979, Y. T. Lo et al have used the cavity model technique to investigate the rectangular, circular, semi-circular, triangular shaped microstrip antenna [5]. C. W. Chew et al. have used the integral equation technique for accurate calculation of resonant frequency of RMA in 1988 for fundamental mode only [6].

L. Shen et al have used the cavity model technique to compute the resonant frequency of Circular Microstrip antenna (CMA) in 1977 [7]. In 1978, S. A Long et al have used the cavity model to analyze investigate the current, radiated power, directivity, gain, different kind of losses, Q-factor and efficiency of CMA [8]. A. Derneryd has used similar approach to investigate the CMA in 1979 [9]. Extensive study on linear and circular polarized CMA has also been reported by J. Huang in 1983 [10].

The resonant behavior, radiation characteristic, input impedance, Q-factor, etc. have also been investigated by simple cavity model technique by K. F. Lee et al. in 1983 for Annular Ring Microstrip Antenna (ARMA) [11-14], Spectral domain technique [16], method of matching expansion [17] etc. have also been reported for those three antennas. It is found that fundamental and higher order mode have been investigated for a single MA only. There is no comparative study and/or analysis between different shaped microstrip antennas. Therefore, we take the opportunity to give a comparative study been Rectangular MA (RMA), Circular MA (CMA) and Annular Ring MA (ARMA).

In this paper, we have presented a comparative study between RMA, CMA and ARMA for first three modes for the first time, hitherto unreported. To compare different shape antennas, we need a common parameter for comparison purpose for this reason all the radiating elements have considered with same area. The relative permittivity ε_r And the thickness of the substrate d is kept constant for all those three antennas. Cavity model technique is applied to investigate those antennas theoretically. Eigenfunction, eigenvalue, resonant frequency and far-field radiation pattern are investigated and compared for all three antennas. Resonant frequencies for first 10 modes of those antennas are compared. Magnetic surface current model is used here to find the far-field radiation patterns. The far-field radiation patterns of those antennas are presented for first three modes.

II. Theoretical Investigation

In this section, theoretical investigation on different shaped microstrip antennas (RMA, CMA, and ARMA) is presented. It is assumed that all antennas have same substrate having relative permittivity ε_r and the thickness of the substrate is d. Magnetic wall model is used to investigate all those antennas.

A. Rectangular Microstrip Antenna

The antenna geometry of the Rectangular MA (RMA) is shown in Fig. 1(a). The RMA has length a and width b. The antenna is placed on xy surface.

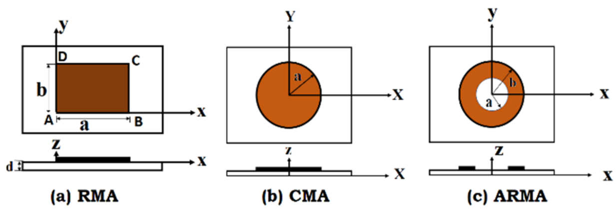

Fig. 1. The geometry of different shaped MAs

For theoretical investigation of RMA, cavity model is applied. To remove the effect of ground plane image theory is applied which results in an isolated RMA having thickness equal to $2d$. All the side walls are modeled here as Perfect Magnetic Conductor (PMC) and the top and bottom surfaces are modeled as Perfect Electric Conductor (PEC). Similar process is also applied for CMA and ARMA also.

The solution of the wave equation $\nabla^2\psi(x,y,z) + k^2\psi(x,y,z) = 0$ is obtained using separation of variable method. After applying the boundary conditions, the eigenfunction $\psi(x,y,z)$ can be expressed as:

$$\psi = A_{mnp}cos(k_x x)cos(k_y y)cosk_z(z-d) \quad (1)$$

where

$$k_x = m\pi/a \quad ; \quad m = 0,1,2,3,4,\ldots..$$

$$k_y = n\pi/b \quad ; \quad n = 0,1,2,3,4,\ldots.$$

$$k_z = p\pi/(2d) \quad ; \quad p = 0,1,2,3,4,\ldots. \quad (2)$$

Here, all terms are carrying their usual meaning.

The resonant frequency (f_r) is found using separation equation $\left(k^2 = {k_x}^2 + {k_y}^2 + k_z^2\right)$ and can be expressed as:

$$f_r = \frac{c}{2\pi\sqrt{\varepsilon_r}}\sqrt{k_x^2 + k_y^2 + k_z^2} \quad (3)$$

To find the far-field radiation patterns, magnetic surface current model is used. The magnetic surface current $\vec{M_S}$ is evaluated as $\vec{M_s} = \vec{E} \times \hat{n}$ along all sidewalls [1] where $\vec{E}$ is the internal electric field and $\hat{n}$ is unit normal outward vector. The Far field zone electric field is given by [18]

$$E_\theta = \frac{-jke^{-jkr}}{4\pi r}[L_\varphi] \quad (4)$$

$$E_\varphi = \frac{jke^{-jkr}}{4\pi r}[L_\theta] \quad (5)$$

$$L_\theta = F_x cos\theta cos\varphi + F_y cos\theta sin\varphi - F_z sin\theta \quad (6)$$

$$L_\varphi = -F_x sin\varphi + F_y cos\varphi \quad (7)$$

where

$$F_x = F_x^{AB} + F_x^{CD}$$

$$F_y = F_y^{BC} + F_y^{DA}$$

$$F_z = 0$$

where

$$F_x^{AB} = C_{xy}A_{mnp} \times \left[\frac{e^{jV_1 a}}{(jV_1)^2 + {k_x}^2}(k_x sin(k_x a) + jV_1\cos(k_x a)) - \frac{jV_1}{(jV_1)^2 + {k_x}^2}\right] \times I_z$$

$$F_y^{BC} = C_{xy}A_{mnp}cos(k_x a)e^{jV_1 a} \times \left[\frac{e^{jV_2 b}}{(jV_2)^2 + {k_y}^2}\left(k_y sin(k_y b) + jV_2\cos(k_y b)\right) - \frac{jV_2}{(jV_2)^2 + {k_y}^2}\right] \times I_z$$

$$F_x^{CD} = -C_{xy}A_{mnp}\cos\left(k_y b\right)e^{jV_1 b} \times \left[\frac{e^{jV_1 a}}{(jV_1)^2 + {k_x}^2}(k_x sin(k_x a) + jV_1\cos(k_x a)) - \frac{jV_1}{(jV_1)^2 + {k_x}^2}\right] \times I_z$$

$$F_y^{DA} = -C_{xy}A_{mnp}\left[\frac{e^{jV_2 b}}{(jV_2)^2 + {k_y}^2}(k_y sin(k_y b) + jV_2\cos(k_y b)) - \frac{jV_2}{(jV_2)^2 + {k_y}^2}\right] \times I_z$$

Here,

$$V_1 = ksin\theta cos\varphi; \quad V_2 = ksin\theta sin\varphi; \quad V_3 = kcos\theta$$

$$I_z = d[(sinc(v_3 + k_z)e^{-jk_z d}) + (sinc(v_3 - k_z)e^{jk_z d})]$$

$$sinc(x) = \begin{cases} 1, & x = 0 \\ \sin(x)/x, & \text{otherwise} \end{cases}$$

B. Circular Microstrip Antenna (CMA)

The geometry of the Circular MA (CMA) is shown in the Fig. 1(b). The radius of the CMA is a. This antenna is also placed on the xy plane like the RMA. To remove the effect of the ground plane, image theory is applied like RMA which results in an isolated source free CMA having thickness of the substrate equal to $2d$. The eigenfunction $\psi(\rho,\varphi,z)$ can be expressed as:

$$\psi = A_{mnp}J_m\left(k_\rho\rho\right)cos(m\varphi)cos[k_z(z-d)] \quad (8)$$

where

$$k_z = p\pi/(2d) \quad ; \quad p = 0,1,2,3,4,\ldots.$$

k_ρ is the root of

$$J'_m\left(k_\rho a\right) = 0 \quad (9)$$

Hence, the resonant frequency (f_r) can be computed from the separation equation $\left(k^2 = k_\rho^2 + k_z^2\right)$ as

$$f_r = \frac{c}{2\pi\sqrt{\varepsilon_r}}\sqrt{k_\rho^2 + k_z^2} \quad (10)$$

To find far field radiation pattern, magnetic surface current is evaluated along the $\rho = a$ and the far zone electric field is evaluated using eq. (4) and (5) where

$$L_\theta = 2dE_o a\, J_m\left(k_{\rho'}a\right)\cos(\theta) \times \left[2\pi m j^{(m-1)}\sin(m\varphi)\frac{J_n(kasin\theta)}{kasin\theta}\right] \times I_z \quad (11)$$

$$L_\varphi = 2dE_o\, a\, J_m\left(k_\rho a\right) \times \left[2\pi\, j^{(m-1)}\cos(m\varphi)J'_m(kasin\theta)\right] \times I_z \quad (12)$$

C. Annular Ring Microstrip Antenna (ARMA)

Fig. 1(c) depicts the antenna geometry of the Annular Ring MA (ARMA). The outer and inner radius of the ARMA are b and a respectively. Applying cavity model technique like RMA and CMA, the eigenfunction ψ can be expressed as:

$$\psi = \left[J_m\left(k_\rho\rho\right){Y'}_m\left(k_\rho a\right) - {J'}_m\left(k_\rho a\right)Y_m\left(k_\rho\rho\right)\right] \times \cos(m\phi)\cos[(z-d)k_z] \quad (13)$$

Here, $k_\rho = X_{mn}/a$ and X_{mn} is the root of eq. 14

$$J'_m(RX_{mn})Y'_m(X_{mn}) - J'_m(X_{mn})Y'_m(RX_{mn}) = 0 \quad (14)$$

Here J_m and Y_m is first and second kind Bessel function respectively and, $R = b/a$.

The resonant frequency is computed from separation equation $k^2 = k_\rho{}^2 + k_z^2$ and can be evaluated as:

$$f_r = \frac{c}{2\pi\sqrt{\varepsilon_r}}\sqrt{k_\rho^2 + k_z^2} \quad (15)$$

In a similar way like RMA and CMA, the far-field pattern is evaluated using magnetic surface current model. The L_θ and L_φ can be expressed as:

$$L_\theta = L_\theta^a + L_\theta^b \quad (16)$$

$$L_\varphi = L_\varphi^a + L_\varphi^b \quad (17)$$

where

$$L_\theta^b = 2dbZ_{mn}^b \cos(\theta)\left[2\pi mj^{\,(m-1)}\sin(m\varphi)\frac{J_n(kbsin\theta)}{kbsin\theta}\right] \times I_z \quad (18)$$

$$L_\varphi^b = 2dbZ_{mn}^b\left[2\pi\, j^{(m-1)}\cos(m\varphi)J_m'(kbsin\theta)\right] \times I_z \quad (19)$$

$$L_\theta^a = -2d\ a\ Z_{mn}^a\ cos\theta\left[2\pi mj^{\,(m-1)}\sin(m\varphi)\frac{J_n(kasin\theta)}{kasin\theta}\right] \times I_z \quad (20)$$

$$L_\varphi^a = -2daZ_{mn}^a\left[2\pi\, j^{(m-1)}\cos(m\varphi)J_m'(kasin\theta)\right] \times I_z \quad (21)$$

Here,

$$I_z = h\left[(sinc(v_3 + \beta_z)e^{-jk_zh}) + (sinc(v_3 - \beta_z)e^{j\beta_zh})\right]$$

$$Z_{mn}^b = J_m(k_\rho b)Y_m'(k_\rho a) - J_m'(k_\rho a)Y_m(k_\rho b)$$

$$Z_{mn}^a = J_m(k_\rho a)Y_m'(k_\rho a) - J_m'(k_\rho a)Y_m(k_\rho a) \quad (22)$$

III. Results And Discussion

In this section, we have given a comparison between the characteristics of RMA, CMA and ARMA. The shapes of those antennas are different. Therefore, we need a common platform for comparison purpose. To make a comparative study between those three antennas, the area of the microstrip antenna is kept same for all antennas. Besides, the relative permittivity ε_r and the thickness of the substrate is d are kept same for all those three antennas. The substrate thickness of all MAs is taken equal to $d = 1.59\ mm$ and dielectric constant is $\varepsilon_r = 2.32$. The radius of the CMA is $60.6\ mm$ and the inner and outer radius of the ARMA are $35mm$ and $70mm$ respective. In case of RMA, the length and width are taken equal to $131.1mm$ and $87.34mm$ respectively. Those dimensions are chosen in such a way that the MAs should have same areas.

A. Resonant frequency

In this section we have done comparison of resonant frequency of RMA, CMA and ARMA keeping their area constant. It is found from Table I that the CMA has higher resonant frequency at fundamental mode compared to RMA and ARMAs whereas ARMA gives lowest resonant frequency at fundamental mode. The fundamental mode occurred for both CMA and ARMA at modal index of $m = 1,\ n = 1$ and $p = 0$ whereas the same occurs at $m = 1,\ n = 0$ and $p = 0$ for RMA.

TABLE I. Comparison of Resonant Frequency(Area = $0.0115m^2$ and $\varepsilon_r = 2.32$)

SL No of Diff Modes	RMA ($b = 1.5\,a$)		CMA Radius = a		ARMA ($b = 2a$)	
	Mode TM_{mnp}^z	***Freq. (GHz)***	***Mode*** TM_{mnp}^z	***Freq. (GHz)***	***Mode*** TM_{mnp}^z	***Freq. (GHz)***
1	TM_{100}^z	0.75	TM_{110}^z	0.95	TM_{110}^z	0.61
2	TM_{010}^z	1.13	TM_{210}^z	1.58	TM_{210}^z	1.20
3	TM_{110}^z	1.35	TM_{020}^z	1.98	TM_{310}^z	1.77
4	TM_{200}^z	1.50	TM_{310}^z	2.17	TM_{410}^z	2.32
5	TM_{210}^z	1.88	TM_{410}^z	2.75	TM_{510}^z	2.84
6	TM_{020}^z	2.25	TM_{120}^z	2.76	TM_{020}^z	2.86
7	TM_{120}^z	2.37	TM_{510}^z	3.32	TM_{120}^z	2.94
8	TM_{310}^z	2.52	TM_{220}^z	3.47	TM_{220}^z	3.16
9	TM_{220}^z	2.71	TM_{030}^z	3.63	TM_{610}^z	3.34
10	TM_{400}^z	3.00	TM_{610}^z	3.88	TM_{320}^z	3.51

It is also found that the RMA supports more modes for a given range of operating frequency. For example, RMA supports 10 modes within 3.00GHz whereas CMA and ARMA support 6 and 7 modes (approx.) respectively as shown in Table I.

- Therefore, RMA will give more flexibility to design an antenna compared to CMA and ARMA in term of frequency selection.
- Besides, ARMA shows fundamental mode at lower frequency. Hence, to design compact antenna, ARMA is preferred over RMA and CMA.

B. Radiation pattern

Far-field radiation patterns of RMA, CMA and ARMA are compared here for first three modes. MATLAB code is written for comparison purpose. E-plane ($\varphi = 0^o$) and H-plane ($\varphi = 90^o$) are computed for all three antennas. After obtaining all three patterns, the maximum value between those three far-field patterns is used to normalize all those patterns.

Radiation pattern for the fundamental mode of those antennas are shown the Fig. 2. The maximum value of those three It is found from Fig. 2 that the RMA has strongest radiation compared to other MAs at $\theta = 0^o$ for both E and H plane. It is also observed that at $\theta = 0^o$, CMA and ARMA have maximum radiation but it is 2dB and 5.5 dB less respectively compared to maximum radiation of RMA in both radiating plane. It is also found that the Half Power Bandwidth (HPBW) of RMA are 98^0 and 86^0 for E-plane and H-plane respectively. In case of CMA and ARMA, the HPBW are same for H-plane (82^o). In case of E-plane, ARMA has larger HPBW (104^o) compared to other MAs in E-plane radiation.

In the case of 1st higher order mode which is shown in the Fig. 3, the RMA produces peak at the broad side direction for whereas CMA and ARMA give a null in the broad side direction. It is also found that the normalized E-plane and H-plane of the ARMA are just overlapped on each-other. The same observation is found for CMA also. In this mode RMA has good HPBW 72^o(E-plane) and 98^o (H-plane) compared to the other MAs.In the case of 2nd higher order mode, all the antennas have a null at $\theta = 0^o$ in both E and H plane power patterns. In the E-plane, RMA and ARMA show 4dB (approx.) and 10dB (appox.) low compared to CMA whereas the same is approx. 12dB both for RMA and ARMA in H-plane.

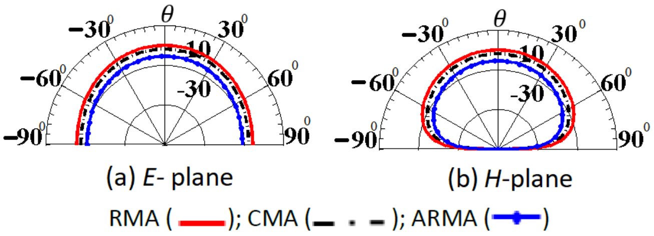

Fig. 2. Normalized far-field at fundamental mode TM_{100}^{z}(RMA) ; TM_{110}^{z} (CMA) and TM_{110}^{z} (ARMA)

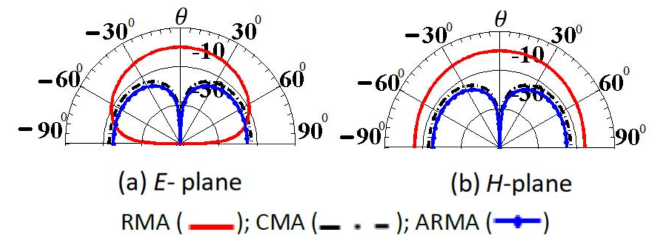

Fig. 3. Normalized far-field at 1st higher order mode TM_{010}^{z} (RMA); TM_{210}^{z} (CMA) and TM_{210}^{z} (ARMA)

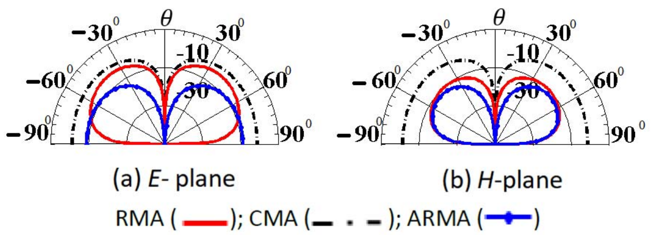

Fig. 4. Normalized far-field at 2nd higher order mode: TM_{110}^{z}(RMA); TM_{020}^{z}(CMA) and TM_{310}^{z} (ARMA)

IV. Conclusion

In this paper, a comparative study between rectangular MA (RMA), circular MA (CMA) and Annular Ring MA (ARMA) is presented for first three modes, for the first time. The area of the radiating patch antenna is kept equal for all three antennas. Cavity model is used here for comparison purpose. From the above study, it is found that.

- The resonant frequency of ARMA is lower than RMA and CMA at the fundamental mode. Hence, ARMA can be used to design compact antenna preferred over RMA and CMA.
- It is also found that the RMA supports more modes for a given range of operating frequency. For example, RMA supports 10 modes within 3.00GHz whereas CMA and ARMA support 6 and 7 modes (approx.) respectively as shown in Table I.
- All the fundamental mode of RMA, CMA and ARMA shows a peak in the broadside direction.
- RMA shows strongest far-field patterns compared to CMA and ARMA at fundamental mode.
- At fundamental mode, ARMA shows wider HPBW (104^{o}) in E-planewhereas the RMA shows wider HPBW (98^{o}) at H-plane.
- The first higher order mode of RMA (TM_{010}^{z}) is a broadside radiating mode whereas the same of CMA (TM_{210}^{z}) and ARMA (TM_{210}^{z}) produce a null in the broadside direction.
- The second higher order mode of RMA(TM_{110}^{z}), CMA (TM_{020}^{z}) and ARMA (TM_{310}^{z}) produce a null in the broad-side direction.
- Therefore, RMA shows two broad-side radiating modes out of first three modes compared to CMA and ARMA.

References

[1] K. F. Lee and K. M. Luk, *Microstrip Patch Antennas*. London:Imperial College Press, 2011.

[2] R. Munson, "Conformal microstrip antennas and microstrip phased arrays," *IEEE Transactions on Antennas and Propagation*, vol. 22, no. 1, pp. 74-78, January 1974.

[3] A. Dernerуd and A. Lind, "Extended analysis of rectangular microstrip resonator antennas," IEEE Transactions on Antennas and Propagation, vol. 27, no. 6, pp. 846-849, November 1979.

[4] A. Derneryd, "A theoretical investigation of the rectangular microstrip antenna element," IEEE Transactions on Antennas and Propagation, vol. 26, no. 4, pp. 532-535, July 1978.

[5] Y. Lo, D. Solomon and W. Richards, "Theory and experiment on microstrip antennas," *IEEE Transactions on Antennas and Propagation*, vol. 27, no. 2, pp. 137-145, March 1979.

[6] W. C. Chew and Q. Liu, "Resonance frequency of a rectangular microstrip patch," IEEE Transactions on Antennas and Propagation, vol. 36, no. 8, pp. 1045-1056, Aug. 1988.

[7] L. Shen, S. Long, M. Allerding and M. Walton, "Resonant frequency of a circular disc, printed-circuit antenna," IEEE Transactions on Antennas and Propagation, vol. 25, no. 4, pp. 595-596, July 1977.

[8] S. A. Long, L. C. Shen and P. B. Morel, "Theory of the circular-disc printed-circuit antenna," *Proceedings of the Institution of Electrical Engineers*, vol. 125, no. 10, pp. 925-928, October 1978.

[9] A. Derneryd, "Analysis of the microstrip disk antenna element," *IEEE Transactions on Antennas and Propagation*, vol. 27, no. 5, pp. 660-664, September 1979.

[10] J. Huang, "A circularly polarized conical pattern from a circular microstrip antenna," Antennas and Propagation Society International Symposium, Houston, TX, USA, 1983, pp. 51-54.

[11] K. F. Lee, J. S. Dahele and K. Y. Ho, "Annular-Ring and Circular-Disc Microstrip Antennas with & without Air Gaps,"*European Microwave Conference*, Nurnberg, Germany, 1983, pp. 389-394.

[12] J. S. Dahele and K. F. Lee, "Characteristics of annular-ring microstrip antenna," Electronics Letters, vol. 18, no. 24, pp. 1051-1052, 25 November 1982.

[13] S. E. El-khamy, R. M. El-Awadi and E. -. A. El-Sharrawy, "Simple analysis and design of annular ring microstrip antennas," IEE Proceedings H - Microwaves, Antennas and Propagation, vol. 133, no. 3, pp. 198-202, June 1986.

[14] Bahl, I. J. and Stuchly, S. S., "Closed□form expressions for computer□aided design of microstrip ring antennas". *Int. J. Microw. Mill.□Wave Computer. Aided Egg,* vol: 2: pp. 144-154, 1992.

[15] S. Ali, Weng Chew and J. Kong, "Vector Hankel transform analysis of annular-ring microstrip antenna,"*IEEE Transactions on Antennas and Propagation*, vol. 30, no. 4, pp. 637-644, July 1982.

[16] A. Bhattacharyya and R. Garg, "Spectral domain analysis of wall admittances for circular and annular microstrip patches and the effect of surface waves," in IEEE Transactions on Antennas and Propagation, vol. 33, no. 10, pp. 1067-1073, October 1985.

[17] Weng Chew, "A broad-band annular-ring microstrip antenna," IEEE Transactions on Antennas and Propagation, vol. 30, no. 5, pp. 918-922, September 1982.

[18] C. A Balanis, *Advance Engineering Electromagnetics*, John Wiley & Sons, New York ,1989